Role of barotropic, baroclinic and combined barotropic-baroclinic instability for the growth of monsoon depressions and mid-tropospheric cyclones

B N GOSWAMI*, R N KESHAVAMURTY+ and V SATYAN
Physical Research Laboratory, Ahmedabad 380 009

* Present address : Department of Meteorology, Massachusetts Institute of Technology, Cambridge, Mass. 02139, USA.

+ Present address : Geophysical Fluid Dynamics Program, Princeton University, P.O. Box 308, Princeton, N.J. 08540, USA.

Abstract. A detailed barotropic, baroclinic and combined barotropic-baroclinic stability analysis has been carried out with mean monsoon zonal currents over western India, eastern India and S.E. Asia. The lower and middle tropospheric zonal wind profiles over western India are barotropically unstable. The structure and growth rate of these modes agree well with the observed features of the mid-tropospheric cyclones. Similar profiles over eastern India and S.E. Asia, however, are barotropically stable. This is attributed to weak horizontal shear, inherent to these profiles. The upper tropospheric profiles, on the other hand, are barotropically unstable throughout the whole region. The features of these unstable modes agree with those of observed easterly waves. The baroclinic and combined barotropic-baroclinic stability analyses show that the baroclinic effects are not important in tropics.

Though the barotropic instability of the mean zonal current seems to be responsible for the initial growth of the mid-tropospheric cyclones, neither barotropic nor baroclinic instability of the mean zonal current seem to explain the observed features of the monsoon depressions.

Keywords. Monsoon depressions ; mid-tropospheric cyclones ; mean zonal flows ; barotropic ; baroclinic instability.

1. Introduction

Monsoon over India is characterised by the intense rainfall in this region during that period. Two of the most important components of the monsoon circulation which are responsible for the extensive rain over the Indian continent are the monsoon depressions and the mid-tropospheric cyclones. The morphological structure and the energetics of the monsoon depressions have been studied rather extensively by many authors (Rao 1976; Krishnamurty *et al* 1975; Keshavamurty 1978a). About two out of three of these depressions form over north Bay of Bengal (Rao 1976) while the rest (one-third) possibly originate from the westward moving perturbations which come from China Sea. These depressions then move west or

79

north westward with a typical phase speed of about 3 m/s. The horizontal scale of these depressions is about 2000–3000 km while the vertical scale is about 10 km (Krishnamurty *et al* 1975). The circulation associated with the monsoon depression seem to be most intense around 700 mb though they extend down to the lower layers. The circulation is cyclonic up to about 300 mb above which the flow is diffluent.

Mid-tropospheric cyclones are disturbances that form in the middle tropospheric east-west shear zone over western India. Unlike monsoon depressions, these disturbances have not been extensively studied. However, one such mid-tropospheric cyclone was studied in detail by Miller and Keshavamurty (1968) with the help of I.I.O.E. aircraft and dropsonde data. These disturbances also have scale-lengths in the range of 2000–3000 km. However, they remain almost stationary and rarely extend down to ground level. The name " mid-tropospheric cyclone " is derived from the fact that they generally remain locked up in the middle troposphere.

During active monsoon epochs, disturbances forming over the north Bay of Bengal coupled with mid-tropospheric cyclones over western India result in well-distributed rainfall over central and western India. At this point we can ask a few important questions, viz., (i) how are these disturbances formed ? (ii) is the mechanism for formation of the monsoon depressions different from that of the mid-tropospheric cyclones ? (iii) once these disturbances are formed, how are they maintained ? It is towards answering the first two questions (partially if not fully !) that the efforts in the present paper will be directed.

The gross features of the mean circulation over western India (73° E) are similar to those over eastern India (80° E or 90° E) with the well-known westerly maximum i n the lower troposphere and easterly jet in the upper troposphere. The transition from lower-level westerlies to upper-level easterlies occurs at about 500 mb. However, if we travel from western India to S.E. Asia (for representative cross-section of the mean monthly zonal winds, we refer to such sections along 73° E, 80° E and 100° E shown by Raman and Ramage 1972) the details of the circulations differ in some respects. For example, the east-west shear zone is more marked over western India and becomes less marked as we go towards S.E. Asia. The east-west shear zone in the middle levels over western India is possibly due to the formation of a heat low over north-west India–Pakistan overlain by an anticyclonic flow in the middle levels. As is seen from these sections, the mean zonal flow U is a function of the latitude y and pressure p which indicates that there are two possible sources of energy for any perturbation to grow, viz., zonal kinetic energy and available potential energy.

An examination of these cross-sections of the mean zonal wind shows the presence of a weak easterly wind between two westerly maxima. Thus, there exists an internal jet and this suggests the possibility of an internal jet instability as the mechanism of growth for the disturbances mentioned above. The *necessary* condition for such an instability, derived by Charney and Stern (1962) and Pedlosky (1964), indicates that the gradient of the potential vorticity of the mean flow on an isentropic surface should vanish somewhere within the channel. The meridional gradient of the potential vorticity $\bar{P}$ is given by

$$\partial \bar{P}/\partial y = \beta - \frac{\partial^2 U}{\partial y^2} - f_0^2 \frac{\partial}{\partial p}\left(\frac{1}{\sigma}\frac{\partial U}{\partial p}\right)$$

$$(\partial \bar{P}/\partial y)_{i,j} = \beta - (U_{i+1} + U_{i-1} - 2U_i)/\triangle y^2 + S_{j-1}\,(U_j - U_{j-2})$$

$$+ S_{j+1}\,(U_j - U_{j+2}). \tag{1}$$

where

$$S_j = f_0^2/(\triangle p^2 \sigma_i)$$

and

$$\sigma_j = -\,(a/\theta)_j\,(\partial\theta/\partial p)_j.$$

In writing the finite difference form for the gradient of potential vorticity in (1), the central difference scheme has been used both in the horizontal and vertical directions. The subscripts i and j represent the ith grid point in the y-direction and the jth level in the vertical, respectively. Using a standard σ-profile for the monsoon atmosphere and using the mean zonal wind profiles, we computed $\partial P/\partial y$ along 73° E, as well as along 80° E. These computations show that $\partial \bar{P}/\partial y = 0$ at several levels around 20° N along 73° E as well as along 80° E. A break-up of $\partial \bar{P}/\partial y$ shows that its vanishing is mainly contributed by β and $-\partial^2 U/\partial y^2$ cancelling each other. This suggests the possible existence of an internal jet instability. However, this is only a necessary condition and not the sufficient condition.

From the observed features of the disturbances one can also derive the energetics of the disturbances, their horizontal and vertical tilt and so on. These features might tell us which instability mechanism *may* be responsible for the growth of these disturbances. For monsoon depressions such detailed analysis has been done by several authors, viz., Keshavamurty (1971), Krishnamurty *et al* (1975), Keshavamurty *et al* (1978a) to name a few. Keshavamurty (1971) showed that monsoon depressions do not have the eastward tilt with height necessary for a baroclinic growth. Therefore, he conjectured that baroclinic instability may not be the initial growth mechanism for the monsoon depressions. Moreover, the momentum transport by the disturbances show that they derive energy from the kinetic energy of the basic flow. This points towards barotropic instability as the possible mechanism for their growth. However, such detailed calculations have not been done for the mid-tropospheric cyclones.

A large number of theoretical studies have been devoted towards figuring out what exactly is the mechanism for the growth of the monsoon disturbances. Noteworthy amongst them are recent studies by Shukla (1974, 1977); Keshavamurty *et al* (1978a, b) and Satyan *et al* (1978). Shukla (1974) used a ten-layer quasigeostrophic model and found only a barotropic mode at 150 mb. He did not find any barotropic modes at lower levels and it is hard to see how the barotropic mode at 150 mb can extend all the way to lower levels. Moreover, as shown by Charney (1969) the vertical coupling in the tropical atmosphere is weak. Therefore, in a later paper, Shukla (1977) invoked CISK as the mechanism of growth for these disturbances. However, it is not easy to see how CISK can operate if a low level convergence is not produced by some other mechanism (say barotropic instability). Satyan *et al* (1978) emphasised that the presence of a global monsoon

wave with its proper phase over Indian subcontinent is essential for the cyclogenesis of the monsoon disturbances. Towards the understanding of the mechanism of growth for the mid-tropospheric disturbances, however, the effort has been limited to a few papers. Mak (1975) proposed that baroclinic instability of the monsoon current over western India with the meridional motion also present, may be the mechanism of growth of the mid-tropospheric cyclones. From Mak's study it appears that the meridional wind required for instability is rather large compared to reality. Carr (1977) made a detailed numerical study of these disturbances and concluded that condensation heating in association with orographic rain is important for their maintenance. It is the intention of this paper to study in detail whether barotropic instability, baroclinic instability or a combination of them is responsible for the growth of these disturbances and whether there exists an essential difference in the mechanism of growth for these two types of disturbances.

In § 2, we present a detailed barotropic stability analysis of the mean zonal current for the month of July over western India, eastern India and S.E. Asia. It is shown in this section that the west Indian mean zonal current at lower levels (up to 500 mb) is susceptible to barotropic instability while the zonal current over S.E. Asia is stable to barotropic perturbations. The reason for this phenomenon lies in the fact that the horizontal shear in the zonal wind reduces considerably as we go from western India to S.E. Asia. The upper level (200 mb) zonal wind, however, is barotropically unstable throughout the whole region. In § 4, we have shown that the zonal wind is always baroclinically stable. In § 3, we have carried out a combined barotropic-baroclinic stability analysis using a two-layer quasigeostrophic model. This analysis yields the same lower and upper tropospheric barotropically unstable modes over western India with marginal modification due to the presence of baroclinicity. Over eastern India and S.E. Asia we again get the upper tropospheric modes only. The barotropically unstable modes in the lower and middle troposphere over western India have structure, growth rate and latitudinal tilt that agree well with observed features of the mid-tropospheric cyclones. Therefore, barotropic instability of the mean zonal current seems to be the initial growth mechanism for these disturbances. In the appendix, we present a series of tests on the validity of our numerical techniques.

2. Barotropic instability of monsoon zonal flow

In § 1, we noted that the potential vorticity of the monsoon zonal flow shows extremum values within the region of interest. We also noted that the vanishing of the gradient of potential vorticity is mainly contributed by the barotropic term. Therefore, in this section, we shall carry out a barotropic stability analysis of the mean monsoon zonal flow.

The formulation is exactly similar to one used by Keshavamurty *et al* (1978a). The linearised quasigeostrophic vorticity equation is studied. By using normal mode analysis the problem is reduced to an eigenvalue problem.

We look for modes characterised by a wave number k for which the phase speed c is complex. The real part of c gives us the phase speed of the disturbances while the imaginary part gives us the growth rate and hence the doubling time for the disturbances. We solve the matrix equation using the efficient numerical algorithm

which gives us the eigenvalue c's. For each eigenvalue it also gives the latitudinal variation of the corresponding eigenvector (in other words, the amplitude and phase distribution of the disturbance with latitude). The amplitude distribution gives us the structure of the disturbance while from the phase diagram we can have an idea of the energetics of the disturbance. Such numerical techniques have been used by many authors (Yanai and Nitta 1968; Green 1960) for stability analysis of atmospheric flows.

We have made a stability analysis for profiles between 850 mb and 200 mb along 73° E, 80° E and 100° E using a one degree grid in the channel between the equator and 30° N. The smoothed profiles used in the numerical computations for 700 mb, 500 mb and 200 mb are shown in figures 1–3. These smoothed profiles have been obtained by plotting climatological mean upper wind data obtained from the India Meteorological Department. At 700 mb we find that the profile along 73° E gives a fast growing mode with doubling time of about 4 days and an eastward phase speed of about 3 m/sec. The scale dependence of the growth rate for the mode is shown in figure 4. It is seen from this figure that the preferred scale is about 2500 km. The profiles along 80° E and 100° E at 700 mb, however, do not show growing modes with appreciable growth rates. At 500 mb, again the profile along 73° E shows a growing mode with doubling time of about 5 days and an eastward phase speed of about 2 m/sec while the profile along 80° E shows only a very slowly growing mode with the shortest doubling time of about 8·2 days. The 500 mb profile along 100° E shows no growing mode. The scale-dependence of these modes at 500 mb is shown in figure 5. In contrast to the lower troposphere, the upper tropospheric profiles (namely that at 200 mb) seem to be always barotropically unstable. The scale-dependence of the 200 mb barotropic modes along 73° E, 80° E and 100° E is shown in figure 6. The maximally growing mode at 200 mb along 73° E has a scale length of about 1800 km while those along 80° E and 100° E have scale lengths of about 2000 km and 2500 km respectively.
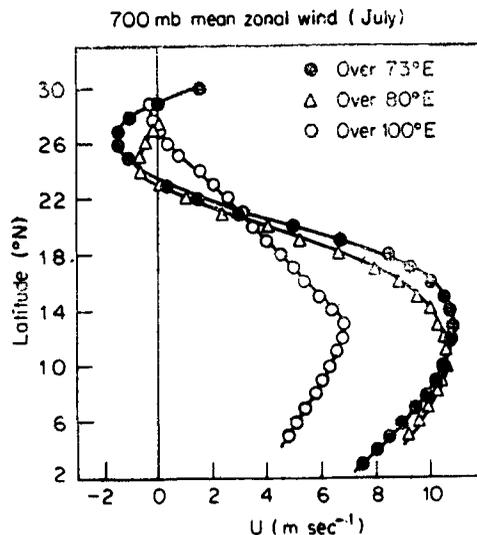

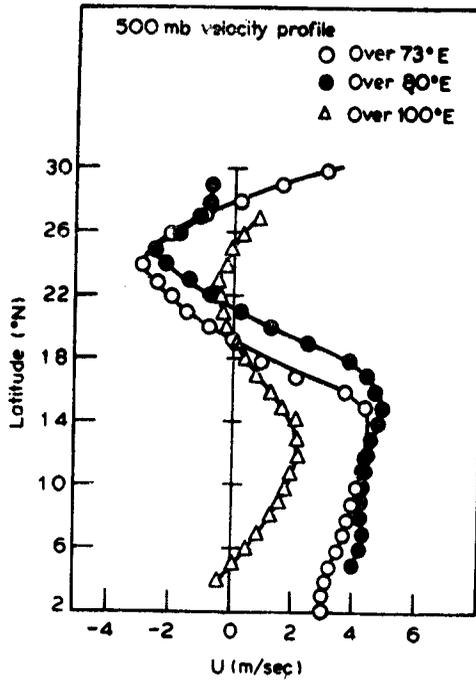**Figure 1.** Smoothed mean zonal wind profile (July) at 700 mb along 73° E, 80° E and 100° E respectively.
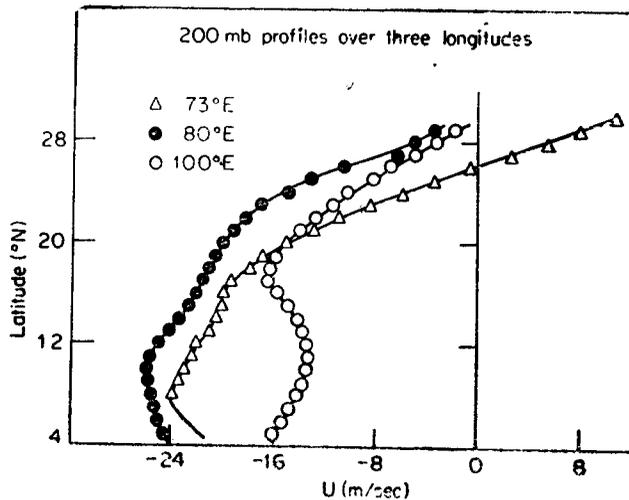
Figure 2. Same as figure 1 at 500 mb.

Figure 3. Same as figure 1 at 200 mb.

Having observed that the lower and middle tropospheric zonal wind profiles are barotropically unstable over western India while they are not barotropically unstable over eastern India and S.E. Asia, we believe that the barotropic instability of the mean zonal flow may be the mechanism of growth for the mid-tropospheric cyclones. With this observation we looked at the unstable modes along
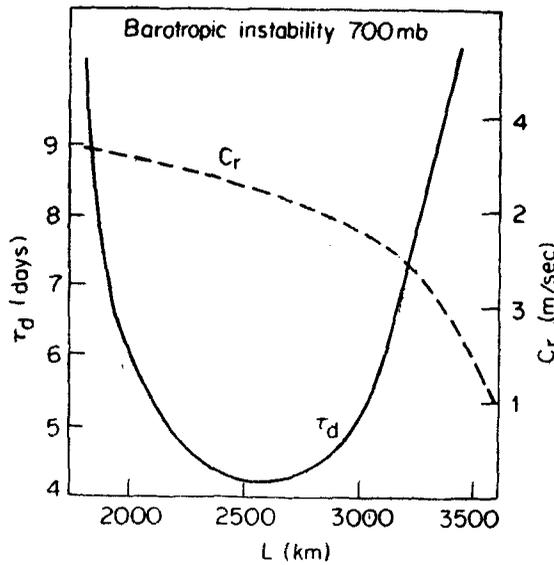
Figure 4. Scale-dependence for the growth rate of the barotropic mode at 700 mb.
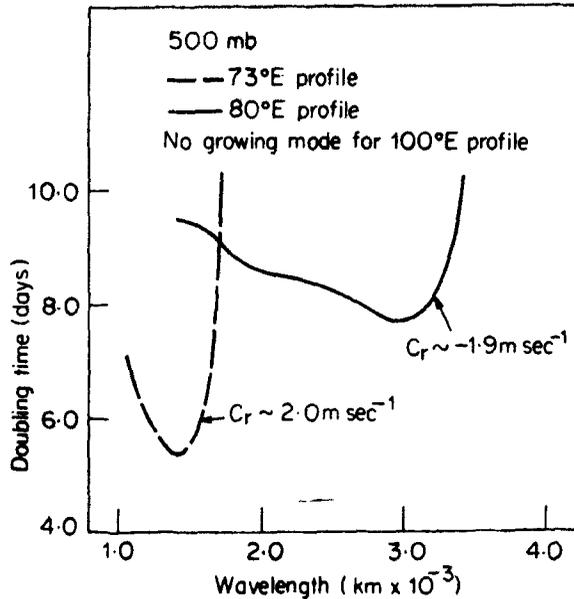

Figure 5. Same as figure 4 at 500 mb.

73° E more carefully. The scale length of these modes agrees well with obser-
vation. We also plotted the amplitude distribution of these modes and they
show realistic structure with maximum amplitude around 20° N. As an example,
the amplitude distribution of the most unstable modes at 700 mb and 200 mb are
shown in figure 7. That these modes are genuine barotropic modes is confirmed
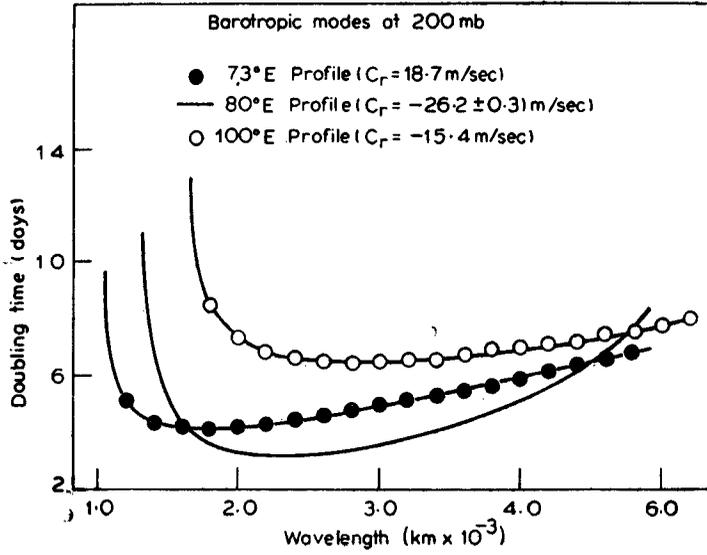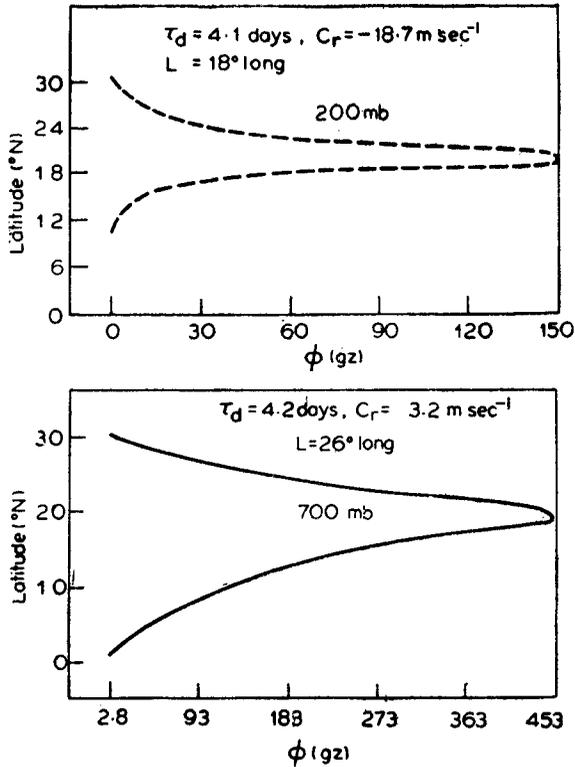
Figure 6. Same as figure 4 at 200 mb.

Figure 7. Amplitude profile of the barotropic modes at 700 mb and 200 mb.

from the fact that the phase speed lies between minimum zonal wind and the critical zonal wind speed (where $\beta - \partial^2 U/\partial y^2 = 0$), which is in agreement with Kuo's (1949) theory.

We then looked at the phase plot of the disturbance which gives us the latitudinal tilt of the disturbance. The lower and middle tropospheric modes have a tilt of the trough (ridge) from NNE to SSW which would be associated with northward transport of westerly momentum. Moreover, the disturbance has maximum amplitude north of the maximum westerly zonal wind. In the equation for the rate of change of eddy kinetic energy (K_E)

$$\partial K_E/\partial t = - \int \overline{u'v'}\frac{\partial U}{\partial y}\, dm \tag{2}$$

where $\overline{u'v'}$ is the momentum transport by the wave and is positive in the present case in the region where $\partial U/\partial y$ is negative. Thus $\partial K_E/\partial t$ is positive. This also suggests that these modes obtained by the numerical method correspond to observed mid-tropospheric cyclones.

The phase speed of the disturbances obtained from this analysis, however, does not agree with observations. We get an eastward phase speed of about 2–3 m/sec while the mid-tropospheric cyclones are almost stationary. This is due to the following reason. The barotropic stability analysis we have used, has no inherent divergence. Hence, these perturbations ride on the basic current and get carried away by them. The amplitude distribution (figure 7) shows that the disturbances have maximum amplitude around $20°$ N. The basic current in this region is westerly and hence the eastward movement of the disturbances. Carr (1977) carried out a detailed numerical simulation and showed that condensational heating in association with orographic rain gave rise to enough divergence to keep these disturbances stationary. For the same reason we always get a westward phase speed for the upper tropospheric disturbances.

Having established that the lower and middle tropospheric mean zonal wind profiles over western India are unstable to barotropic perturbations whose structure agrees well with observed mid-tropospheric cyclones, one can ask the following question: How critically do these disturbances depend on the horizontal shear in the velocity profile? To answer this question we repeated the experiment at 700 mb with reduced velocity shear. We multiplied the 700 mb profile along $73°$ E shown in figure 1 by $0 \cdot 9$, $0 \cdot 8$ and so on. This reduced the magnitude of the velocity keeping the position of the jets unaltered. Essentially this reduced the average shear in the velocity profile. The results of these experiments are shown in figures 8 and 9. As is seen from figure 8, the growth rate drastically reduces as we reduce the shear to about $0 \cdot 7$ times the normal July shear along $73°$ E. In figure 10 we have plotted the doubling time corresponding to the fastest growing mode as a function of average velocity shear.

At this point we can ask another question. What is so special about the July mean zonal profile over western India? In other words, are the June and August profiles in the lower and middle troposphere over western India equally cyclogenetic? To answer this question, we carried out another series of experiments with the June and August profiles. The mean zonal wind profiles at 700 mb along $73°$ E for June, July and August and the scale-dependence of the barotropically
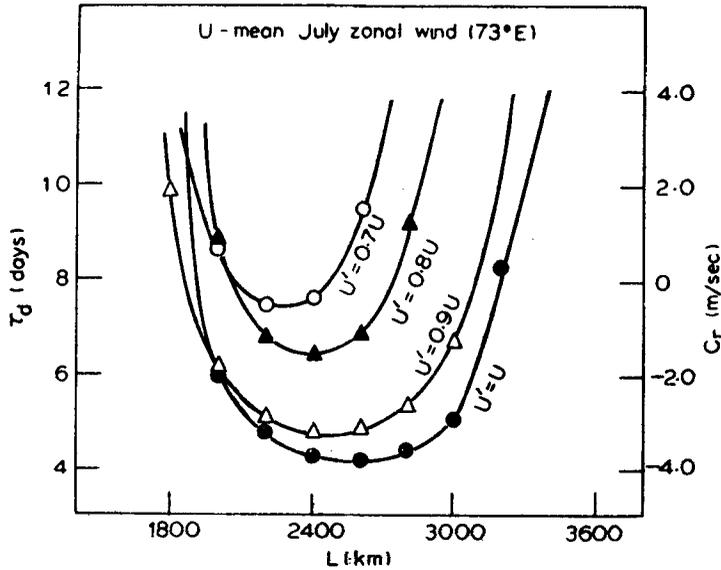
Figure 8. Scale-dependence of the barotropic mode at 700 mb (73° E) for reduced shears.
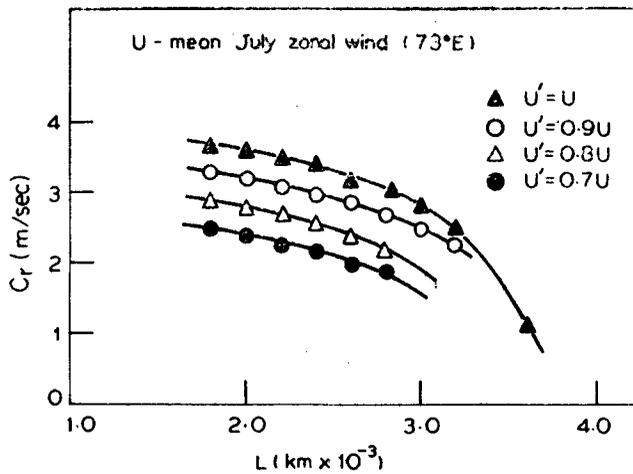

Figure 9. Scale-dependence of the phase velocity corresponding to the mode described in figure 8.

growing modes yielded from these profiles are shown in figures 11 and 12 respectively. From figure 11 it is clear that the jet structure is more prominent in July compared to those in June and August. As seen from figure 12, the July profile is more unstable to barotropic perturbations compared to the other two profiles. Apart from having slower growth rates in the months of June and August, the barotropically unstable modes in these months have maximum amplitude around

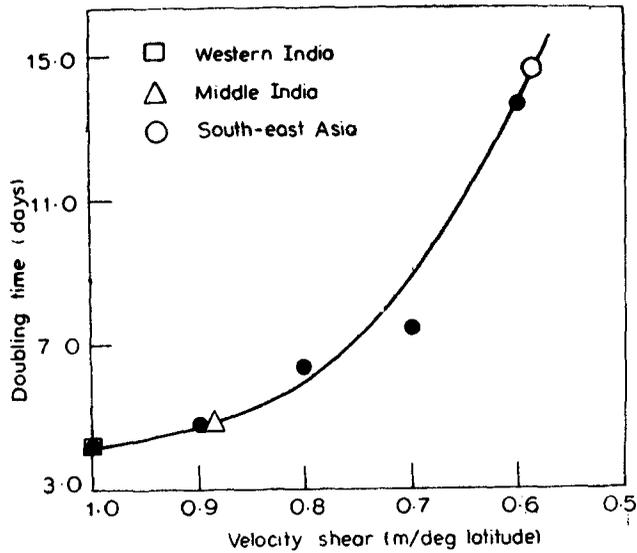**Figure 10.** Doubling-time versus average horizontal shear of the zonal wind for barotropic instability. The points in this figure are obtained from the numerical experiments and the solid line is the mean fit through these points.
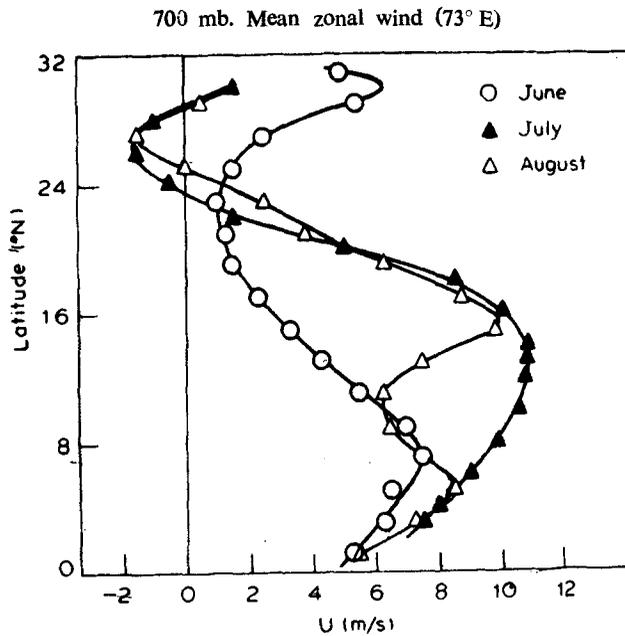

Figure 11. Mean zonal wind at 700 mb (73° E) for the months of June, July and August.

25° N. In this region, the basic zonal wind profile is easterly and hence the westward movement for these modes.
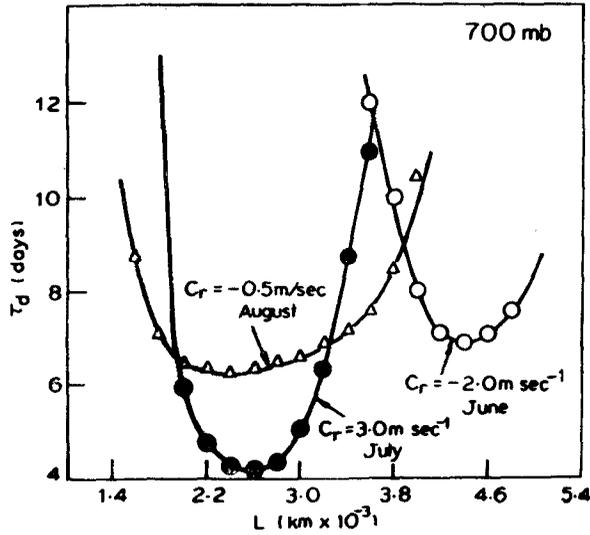
Figure 12. Scale-dependence of the barotropic modes obtained by using U-profiles shown in figure 11.

We also experimented with zonal wind profiles at 600 mb along 73° E for June, July and August. We arrive at conclusions similar to ones obtained for profiles at 700 mb, namely, the July profile has more horizontal shear and hence is more barotropically unstable compared to the profiles in June and August.

3. Combined barotropic-baroclinic instability of the monsoon zonal flow

As we have seen in § 1, the Charney–Stern (1962) condition for possible existence of an internal jet instability is satisfied by the basic flow over western India. Hence we have carried out a combined barotropic-baroclinic stability analysis of the zonal flow using a two-level quasi-geostrophic model with a view to see how the barotropic instabilities are modified by the presence of the baroclinic effects.

As the results to be presented in this section are based on the use of quasi-geostrophic equations, a few words on the rationale for their use are in order at this point. The quasigeostrophic equations can be derived from the primitive equations if the following conditions are satisfied (Phillips 1963),

(1) $R_0 \equiv U/f_0 L \ll 1$,

(2) $R_0^2 R_i \equiv R_0^2 \left[\dfrac{g \frac{\partial}{\partial z} (\ln \theta)}{(\partial U/\partial z)^2} \right] \sim 1$,

and (3) $L_y/a \ll 1$,

where R_0 is the Rossby number, R_i is the Richardson number, L_y is the north-south scale for the motions under consideration, U is the velocity scale, L is the

east-west length scale and a is the radius of the earth. Obviously, the quasi-geostrophic equations are not valid very close to the equator due to the vanishing of f_0. However, we intend to study the wave disturbances in a β-plane model centered around $\phi = 20°$ N. Thus, using $U \sim 10$ m/sec, $L \sim 1000$ km, we get $R_0 \sim 0.2$. Also

$$R_0^2 \, R_i \sim \frac{g\,(z_1 - z_3)}{f_0^2\,L^2}\left(\frac{\theta_1 - \theta_3}{\theta_2}\right).$$

Using Jordan's (1958) data for standard static parameters we get $R_0^2 \, R_i \sim 1.1$. Therefore, by using the quasigeostrophic equations we can hope to capture at least the dominant features of the tropical disturbances. The third condition shall be tested *a posteriori*. This condition requires that the tropical disturbances be confined to rather a small latitudinal band. As will be seen later in this section, the disturbances have y-scale of the order of 2000 km.

Although the foregoing discussions suggest that we can expect to study the salient features of tropical disturbances by using the quasigeostrophic equations, we would like to point out, however, that this is only an initial attempt to study these disturbances. These studies will be extended later by using the more general primitive equations.

$$
\begin{array}{lcl}
 & P & Level \\
 & \omega_0 = 0 & \\
(\text{mb}) \quad 0 & \rule{3cm}{0.4pt} & 0 \\
250 & \rule{3cm}{0.4pt} & 1 \qquad \uparrow \\
500 & \rule{3cm}{0.4pt} & 2 \qquad \triangle P \\
750 & \rule{3cm}{0.4pt} & 3 \qquad \downarrow \\
1000 & \rule{3cm}{0.4pt} & 4 \\
 & \omega_4 = \omega_f &
\end{array}
$$

The perturbation potential vorticity equations at levels 1 and 3 are

$$\left(\frac{\partial}{\partial t} + U_1 \frac{\partial}{\partial x}\right)\left\{\zeta_1' + \frac{S_2}{f_0}(\phi_3' - \phi_1')\right\} + v_1'\left\{\beta - \frac{\partial^2 U_1}{\partial y^2} - S_2(U_3 - U_1)\right\}$$

$$= -\frac{R}{C_P}\frac{\triangle p}{p_2}\frac{S_2}{f_0}\dot{Q}_2',\tag{3}$$

and

$$\left(\frac{\partial}{\partial t} + U_3 \frac{\partial}{\partial x}\right)\left\{\zeta_3' - \frac{S_2}{f_0}(\phi_3' - \phi_1')\right\} + v_3'\left\{\beta - \frac{\partial^2 U_3}{\partial y^2} + S_2(U_3 - U_1)\right\}$$

$$- \frac{f_0}{\triangle p}\omega_4' = \frac{R}{C_P}\frac{\triangle p}{p_2}\frac{S_2}{f_0}\dot{Q}_2',\tag{4}$$

where S_2 has the same definition as used in section 1 and $\dot{Q}_2'$ is the rate of non-adiabatic heating at level 2. If we divide the channel in the y-direction into n-latitudes (as was done in § 2) and if we look for solutions of the type $\phi' \sim \phi(y) \times \exp\{ik(x - ct)\}$ the equations corresponding to jth latitude can be written as

$$(U_j^1 - C)\{(\phi_{j+1}^1 + \phi_{j-1}^1 - 2\phi_j^1)/\triangle y^2 - k^2\phi_j^1 + S_2(\phi_j^3 - \phi_j^1)\}$$

$$+ \phi_j^1\{\beta - (U_{j+1}^1 + U_{j-1}^1 - 2U_j^1)/\triangle y^2 - S_2(U_j^3 - U_j^1)\}$$

$$= (i/k)(R\triangle p/C_{p2})S_2\dot{Q}_2'\exp\{-ik(x - ct)\},\tag{5}$$

and $(U_j^3 - C)\{(\phi_{j+1}^3 + \phi_{j-1}^3 - 2\phi_j^3)/\triangle y^2 - k^2\,\phi_j^3 - S_2(\phi_j^3 - \phi_j^1))\}$

$\qquad + \phi_j^3\{\beta - (U_{j+1}^3 + U_{j-1}^3 - 2U_j^3)/\triangle y^2 + S_2(U_j^3 - U_j^1)\}$

$\qquad = -\{(i/k)(R\triangle p/C_P p_2)\,S_2\,Q_2' + (i/k)(f_0^2\,\omega_4'/\triangle p)\}$

$\qquad \times \exp\{-ik(x - ct)\}.$ \hfill (6)

Thus, we have $2n$ equations in the $2n$ unknowns (ϕ_j', ϕ_j^3). For a nontrivial solution, the determinant of the matrix of coefficients must vanish. In matrix notation again we can write

$$(P - cQ)\,(\phi) = 0,$$

or $(PQ^{-1} - cI)\,(Q\phi) = 0.$ \hfill (7)

Once again the problem reduces to finding the eigenvalues of the matrix PQ^{-1} and eigenvectors $Q\phi$ and hence ϕ. This we do numerically.

The channel chosen in the y-direction for this numerical study is between $10°\,N$ and $30°\,N$ with a one-degree grid. The boundary conditions used are $\omega = 0$ at the top boundary and ω is the frictional ω_f at the bottom boundary and $\phi^1 = \phi^3 = 0$ at the southern and northern boundaries. In this part of the study the cumulus heating is assumed to be absent.

The fastest growing modes obtained from this stability analysis using velocity profiles along $73°\,E$ are listed in table 1. It yields the same two modes, one in the lower middle troposphere and one in the upper troposphere earlier obtained in the barotropic stability analysis (see § 2). Figures 13 and 14 show the scale-dependence of the growth rate of the lower and upper tropospheric modes. The amplitude distributions of the most unstable modes are shown in figure 15. Thus, these are essentially seen to be barotropically unstable modes which are not very much affected by the presence of the baroclinic effects.

We have also experimented with the two-level model 700 mb and 200 mb velocity profiles along $80°\,E$ and found that there is no growing mode in the lower troposphere while the same upper tropospheric mode appears with a slightly slower growth rate. The maximally growing upper tropospheric mode has wavelength of about 3000 km. This mode moves westward with a phase speed of about 25 m/sec and a doubling time of $6\cdot2$ days.

Table 1. Fastest growing modes obtained from combined barotropic–baroclinic stability analysis without heating.

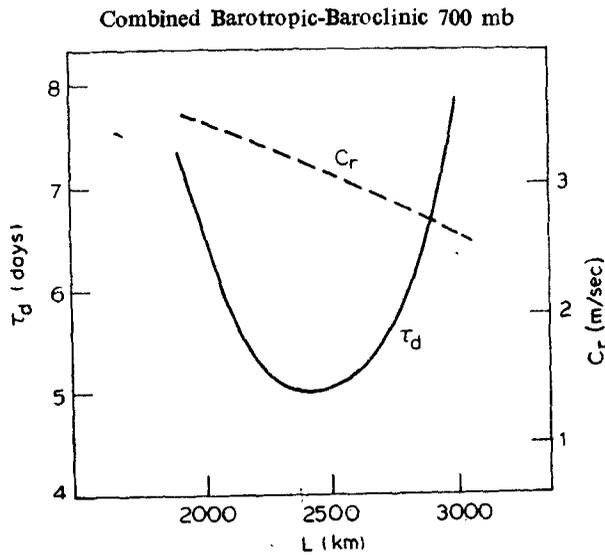| Mode	Position in the vertical	Wave-length (deg. long.)	C_r (m. sec^{-1})	Doubling time (days)
1	Lower troposphere	24	$3\cdot2$	$5\cdot0$
2	Upper troposphere	18	$-18\cdot6$	$4\cdot2$

Combined Barotropic-Baroclinic 700 mb

Figure 13. Scale-dependence of the lower tropospheric mode obtained from the combined model.
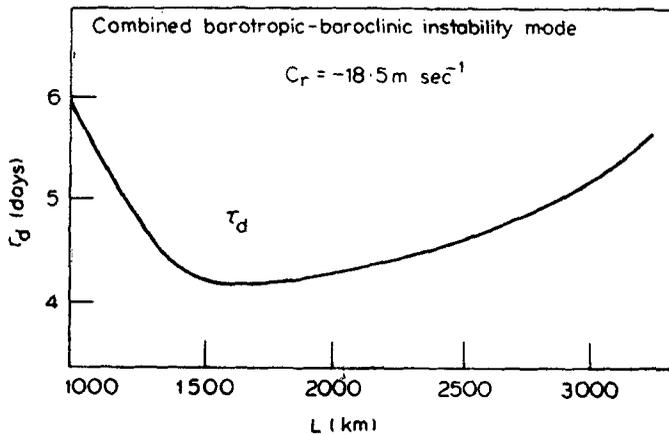

Figure 14. Scale-dependence of the upper tropospheric mode obtained from the combined model.

The growing modes have slightly slower growth rates in the combined model as compared to the barotropic case. This feature was also observed by Shukla (1974). These results would remind one of Charney's (1969) conclusion from his scale analysis in the tropics, that there is no large vertical coupling in the tropics and the tropical atmosphere is quasibarotropic in the absence of deep cumulus convection.

4. Stability of the monsoon zonal flow with only vertical shear

In the previous section the stability analysis with a two-level quasigeostrophic model showed that baroclinic effects may not be important in the tropics. To confirm
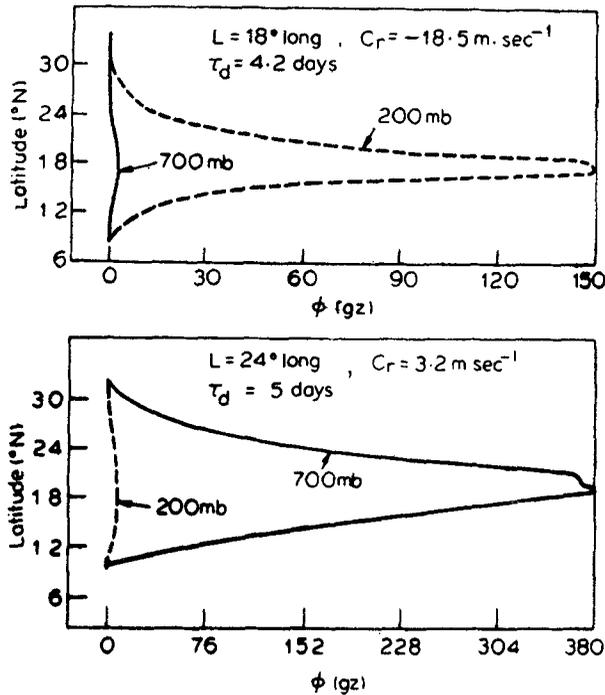
Figure 15. Amplitude profiles of the combined barotropic-baroclinic modes.

this result we carried out a stability analysis of the mean zonal flow with only vertical shear. The methodology, formulation and the boundary conditions used are the same as Keshavamurty *et al* (1978a).

We used the observed $U(p)$ profiles along 73° E and 80° E around 20° N and a mean $\sigma(p)$ profile for the mean monsoon atmosphere in a 20-level model. In the lower levels the velocity profiles were modified such that it has the same speed as the maximum speed above the friction layer. In other words the reduction of speed due to friction is not considered. Both these profiles did not show any unstable modes. Only when the zonal wind speed was increased to 1·5 times the normal speed at all levels, they showed slowly growing unstable modes with the shortest doubling time of about 10 days and having maximum amplitude in the upper troposphere. In other words, the vertical shear in the monsoon zonal wind has to be increased more than 1·5 times for the baroclinic instability to be important.

5. Discussions and conclusions

We have carried out a series of barotropic, baroclinic and combined barotropic-baroclinic stability analyses of monsoon zonal flow over western India, eastern India and S.E. Asia. From this study, the following interesting features have emerged:

(i) The zonal flow in the lower and middle troposphere over western India is barotropically unstable. The most unstable mode in the lower troposphere in this

region has a wavelength of about 26° long. and a doubling time of about 4·2 days. The wavelength, period and the structure of these disturbances agree well with observed features of the mid-tropospheric cyclones. However, the zonal flow at lower and middle troposphere over eastern India and S.E. Asia are found to be barotropically stable.

(ii) The upper tropospheric profiles (200 mb), on the other hand, are barotropically unstable right from western India to S.E. Asia. These upper tropospheric barotropically unstable modes are believed to correspond to observed easterly waves.

(iii) The monsoon zonal flow does not yield any baroclinically unstable modes. Only when the vertical shear is increased to 1·5 times the normal value do we obtain a baroclinically growing mode in the upper troposphere.

In the combined barotropic-baroclinic stability analysis the same modes obtained in the barotropic analysis again come out only with marginal changes. In other words, baroclinic effects do not significantly modify these modes.

Thus, we believe that the barotropic instability of the zonal current is the initial growth mechanism for the mid-tropospheric cyclones. Condensational heating in association with orographic rain is expected to be important for their mainte- nance. However, neither barotropic instability nor baroclinic instability nor a combination of them can explain the initial growth for the monsoon depressions. What have we missed in this analysis? Throughout this analysis we have consi- dered only the zonal component of the monsoon flows. The observed monsoon flow is seen to have an appreciable meridional component also. In fact, from ana- lysis of global data, the global picture of the monsoon can be described as a sta- tionary wave of wave number two (global monsoon) superimposed on the mon- soon zonal current (Krishnamurty 1971). Can the global monsoon have a signi- ficant contribution on the cyclogenesis of the monsoon depressions? This question was recently examined by us (Satyan *et al* 1978) in a stability analysis of the com- bined system. Growing modes in the lower troposphere are found whose features correspond well to observed features of the monsoon depressions.

Moreover, the role of conditional instability of second kind (CISK) in the forma- tion and maintenance of the monsoon depressions has not been fully understood so far. The main difficulty with the CISK mechanism formulated by Charney and Eliassen (1964) has been that it gives largest growth rate for the smallest scale disturbances. However, recently Chao (1978) using the Arakawa–Schubert (1974) theory for cumulus convection showed that with this formulation, the CISK mechanism does give maximum growth for scale length of several hundred kilo- meters. In this case the smaller scale waves are damped. The reason being that, for smaller scale disturbances, the frictionally induced vertical velocity decreases with height so rapidly that the resulting cumulus convection is not strong enough for the CISK mechanism to operate. This result makes us believe that the CISK mechanism may, after all, be important for the growth and maintenance of the monsoon depressions.

Appendix

Tests on the validity of numerical methods used

As referred to in § 2 and explicitly discussed in § 4, we reduced our problem to solving n (or $2n$ as the case may be) simultaneous equations for n (or $2n$) unknowns. Then we reduced the problem to a eigenvalue problem and solved for the eigenvalues and eigenfunctions by using a powerful numerical algorithm. In this section we shall carry out two different types of tests on the validity of results obtained by using this numerical method. The first test deals with finding an upper limit on the step size in y. The second deals with comparing results obtained by our method for a given $U(y)$ profile for which some analytical results are available. Since the numerical methods used in both the barotropic and combined barotripic–baroclinic stability analysis are the same, we shall confine ourselves to the barotropic case for carrying out these tests.

In order to see the effect of the numerical errors introduced through the finite difference schemes, we first selected a coarse grid with $\triangle y = 333$ km and carried out the barotropic stability analysis with observed U-profile at 700 mb along 73° E. We then repeated the experiment with finer and finer mesh sizes, namely, with $\triangle y = 222$ km, $\triangle y = 167$ km, $\triangle y = 111$ km and $\triangle y = 56$ km. The results of these runs are shown in table 2. τ_d in table 2 denotes the doubling time for the growing wave. For $\triangle y = 333$ km and 222 km, no growing mode appears for 500 km $\leqslant \lambda \leqslant 4000$ km. Even for $\triangle y = 167$ km, the numerical errors seem to be very large. Only when $\triangle y \leqslant 111$ km the results are consistent with decrease in $\triangle y$. Thus, one degree mesh size seems to be the upper limit in $\triangle y$ one can use in such stability analysis.

Table 2. Results of the barotropic run with U-profile at 700 mb along 73° E with various grid sizes.

Wavelength λ (km)	$\triangle y = 0 \cdot 5$ deg. lat.		$\triangle y = 1 \cdot 0$ deg. lat.		$\triangle y = 1 \cdot 5$ deg. lat.	
	C_r (m/sec)	τ_d (days)	C_r (m/sec)	τ_d (days)	C_r (m/sec)	τ_d (days)
1600	3·5	..	..	..	..	..
1800	3·5	5·9	3·7	27·8	..	..
2000	3·5	5·0	3·6	6·4	..	..
2200	3·4	4·5	3·5	5·0	..	..
2400	3·3	4·3	3·4	4·5	..	..
2600	3·2	4·2	3·3	4·4	3·3	..
2800	3·0	4·2	3·1	4·4	3·3	12·3
3000	2·9	4·5	3·0	4·6	3·2	9·5
3200	2·7	4·9	2·8	5·1	2·9	9·6
3400	2·5	5·6	2·6	6·0	2·8	12·6
3600	2·3	6·9	2·3	8·5	2·7	..
3800	2·1	9·7	1·9	..	..	..
4000	2·0	..	..	..	..	..

The large errors in the result for $\triangle y \geqslant 167$ km may be due to the following reason. The distance between the easterly and westerly jet maxima in the mean monsoon zonal wind profiles vary from 12–13 degree latitude. When $\triangle y \geqslant 1 \cdot 5°$ latitude, this portion of the velocity profile is represented only by a few points. Hence, one of the important terms, namely, $\partial^2 U/\partial y^2$ is not properly represented by the finite difference formulae (central difference scheme used here). We think this to be one of the major sources of error and may be one of the reasons for poor performances with $\triangle y > 167$ km. Therefore, we used one degree latitude grid throughout all our calculations.

References

Arakawa A and Schubert W H 1974 *J. Atmos. Sci.* **31** 674

Carr F H 1977 Paper presented at the Int. Symp. on Monsoons, New Delhi, March 1977

Chao W, Cheng-Wen 1978 *A study of CISK and a numerical simulation of ITCZ and of easterly waves* Ph.D. Thesis, University of California, Los Angeles

Charney J G 1969 *J. Atmos. Sci.* **26** 182

Charney J G and Stern M C 1962 *J. Atmos. Sci.* **19** 159

Charney J G and Eliassen A 1964 *J. Atmos. Sci.* **21** 68

Green J S A 1960 *Q. J. R. Met. Soc.* **86** 237

Haltiner C J 1963 *Tellus* **15** 230

Jordan C L 1958 *J. Meteor.* **15** 91

Keshavamurty R N 1971 *On the maintenance of the mean Indian South West monsoon circulation and the structure and energetics of the monsoon disturbances*, Ph.D. Thesis, Mysore University, India.

Keshavamurty R N, Asnani G C, Pillai P V and Das S K 1978a *Proc. Indian Acad. Sci.* (Earth Planet. Sci). **A87** 61

Keshavamurty R N, Satyan V and Goswami B N 1978b *Nature* (*London*) **274** 576

Krishnamurty T N 1971 *J. Atmos. Sci.* **28** 1342

Krishnamurty T N, Kanamitsu M, Godbole R, Chang C B, Carr F and Chow J H 1975 Report No. 75-3, Dept. of Meteorology, Florida State University.

Kuo H L 1949 *J. Meteor.* **6** 105

Mak Man-Kin 1975 *J. Atmos. Sci.* **32** 2246

Miller F R and Keshavamurty R N 1968 *I.I.O.E. Met. Monograph-1* (East West Centre Press, Honolulu, Hawaii, U.S.A.)

Pedlosky J 1964 *J. Atmos. Sci.* **21** 201

Phillips N A 1963 *Rev. Geophys.* **1** 123

Raman C R V and Ramage C S 1972 *Meteorological Atlas of the International Indian Ocean Expedition* (NSF, Washington, D.C.)

Rao Y P 1976 *Meteorological Manograph* 1/1976 (India Meteorological Department, New Delhi)

Satyan V, Keshavamurty R N and Goswami B N 1978 *Proc. IUTAM/IUGG Symposium on Monsoon Dynamics*, December 1977, New Delhi (Cambridge : University Press)

Shukla J 1974 Paper presented in the MONEX meeting in Princeton

Shukla J 1977 Paper presented in the International Symposium on Monsoons, New Delhi

Yanai M and Nitta T 1968 *J. Met. Soc. Jpn.* **46** 389